

PACS numbers: 68.55.J-, 78.20.Ci, 78.30.-j, 78.40.-q, 78.67.Sc, 81.40.Tv, 82.35.Np

## Structural and Optical Characteristics of PVA/SnO<sub>2</sub>/MnO<sub>2</sub> Nanocomposites for Optical Devices

Saad Abbas Jasim<sup>1</sup>, M. Jawad K<sup>1</sup>, Olaa H. Altemeemi<sup>2</sup>,  
Majeed Ali Habeeb<sup>1</sup>, and Halah Mohammed<sup>1</sup>

<sup>1</sup>College of Education for Pure Sciences,  
Department of Physics,  
University of Babylon,  
Hillah, Iraq

<sup>2</sup>College of Engineering,  
Department of Mechanical Engineering,  
Wasit University,  
Wasit, Iraq

In this research, different concentrations of manganese dioxide (MnO<sub>2</sub>) and tin dioxide (SnO<sub>2</sub>) are composed with polyvinyl alcohol (PVA) to form the PVA/MnO<sub>2</sub>/SnO<sub>2</sub> films. The optical images demonstrate surface structure and morphological characteristics of the prepared films. The FTIR of PVA/SnO<sub>2</sub>/MnO<sub>2</sub> nanocomposites manifest the obvious broad peaks at 3264 and 3242 cm<sup>-1</sup> due to –OH groups and at 2020 cm<sup>-1</sup> due to stretching vibrations. The optical characteristics of PVA/MnO<sub>2</sub>/SnO<sub>2</sub> films are recorded by means of UV–Vis spectroscopy. The band gap is reduced from 3.73 eV to 2.95 eV for PVA/SnO<sub>2</sub>/MnO<sub>2</sub> nanocomposites, and the absorbance is increased with the increasing of SnO<sub>2</sub>/MnO<sub>2</sub> added to PVA. The optical conductivity also is increased with the increasing of incident photon energy. These results open a good opportunity for applications in different devices such as energy storage systems and optoelectronics devices.

У цьому дослідженні різні концентрації діоксиду Мангану (MnO<sub>2</sub>) та діоксиду Стануму (SnO<sub>2</sub>) комбінували з полівініловим спиртом (PVA) для утворення плівок PVA/MnO<sub>2</sub>/SnO<sub>2</sub>. Оптичні зображення продемонстрували структуру поверхні та морфологічні характеристики одержаних плівок. ІЧ-спектроскопія на основі Фур'є-перетвору (FTIR) для наноконкомпозитів PVA/SnO<sub>2</sub>/MnO<sub>2</sub> показала чіткі широкі піки біля 3264 та 3242 см<sup>-1</sup>, зумовлені групами –ОН, і біля 2020 см<sup>-1</sup>, зумовлені валентними коливаннями. Оптичні характеристики плівок PVA/MnO<sub>2</sub>/SnO<sub>2</sub> були зареєстровані за допомогою спектроскопії УФ-видимого діяпазону. Ширина забороненої зони зменшилася з 3,73 еВ до 2,95 еВ для наноконкомпозитів PVA/SnO<sub>2</sub>/MnO<sub>2</sub>, а вбирання збільшувалося зі збільшенням вмісту

частинок  $\text{SnO}_2/\text{MnO}_2$ , що додавалися до PVA. Оптична провідність також збільшувалася зі збільшенням енергії падних фотонів. Одержані результати відкривають гарну можливість для застосувань у різних пристроях, таких як системи накопичення енергії й оптоелектронні прилади.

**Key words:** nanocomposites, structural and optical properties, optical devices.

**Ключові слова:** наноккомпозити, структурні й оптичні властивості, оптичні прилади.

*(Received 12 March, 2024)*

## 1. INTRODUCTION

The contribution of nanoadditives into polymeric material has the ability to create composite polymeric material with specialized applications [1, 2]. These composites have found use in a various technological applications, such as supercapacitors and optoelectronics [3, 4]. Composite materials with special optical and electrical features are applied as substances for various devices [5, 6]. As a result of gathering polymers' machinability, endurance, and other features, composite films have very important practical applications [7, 8].

Metal oxides have implicit uses in optoelectronic devices beside the electrical efficiency [9]. Because of its storage capability,  $\text{MnO}_2$  has deserved the attention of nanostructured-materials' researchers [10, 11]. Various industries have taken an interest in utilizing  $\text{MnO}_2$  in sensors, battery, and optoelectronics applications [12, 13]. PVA is a polymer that features a carbon chain and hydroxyl group. The PVA polymer has outstanding characteristics such as humidity, water absorption, and being easily produced, that has motivated further studies with this substance [14, 15]. The introduction of  $\text{MnO}_2$  and  $\text{SnO}_2$  improves the structural and chemical modifications in the composite features [16]. Dispersed nanoscale  $\text{MnO}_2$  and  $\text{SnO}_2$  are significantly having great effectiveness than at microscale of the same materials [17, 18]. More susceptibility to deterioration with dispersal homogeneity is also provided with  $\text{MnO}_2$  and  $\text{SnO}_2$  [19, 20]. The developing of electrical pathways throughout composite materials and electron transition through electrical pathways are the most important features of the conductivity processing, which are maximized [21, 22]. PVA can be exploited as an excellent-bonded material with the filler to form the polymer composites [23, 24].

The aim of this work is to improve the optical and structural behaviour of  $\text{PVA}/\text{MnO}_2/\text{SnO}_2$  for application of these films in differ-

ent devices, *e.g.*, as energy-storage ones.

## 2. METHODOLOGY

The MnO<sub>2</sub> and SnO<sub>2</sub> powder (purity of 99.95% and average size of 25–40 nm) was produced from Nanografi Nano Technology Company (Darmstadt, Germany). The PVA powder (with molecular weight of 29,000–69,000 g/mole and by 87.90% hydrolysed) was given by Sigma–Aldrich Company (Darmstadt, Germany).

The solution casting method was chosen for making polymer films due to that it involves a simple preparation, inexpensive, allows for the very precise management of composite composition, and produces highly uniform nanocomposite films. Firstly, 1.0 g of PVA was dissolved in 35 mL of deionized water with magnetic stirring for 35 minutes; after that, different amounts of MnO<sub>2</sub> and SnO<sub>2</sub> (1, 2, and 3 wt.%) were added to PVA. The PVA/MnO<sub>2</sub>/SnO<sub>2</sub> solution was then poured into a glass Petri dish and allowed to air dry at room temperature for 72 hrs.

The chemical changes were studied with FTIR (Shimadzu FTIR, Tracer 100, Kyoto, Japan) at the wavenumbers of 410–3900 cm<sup>-1</sup>. In order to determine the morphology and geometric shape of the films and the distribution of nanoparticles in the polymer, optical image had been used.

The absorption spectrum has been recorded at room temperature in the wavelength range 200–800 nm by using the double-beam spectrophotometer (Shimadzu UV–1800 Å). A computer program was employed to obtain the optical constants for PVA/SnO<sub>2</sub>/MnO<sub>2</sub> films: absorbance, absorption coefficient, refractive index, and energy gap.

The following relation was used to get the absorption coefficient ( $\alpha$ ) [25, 26]:  $\alpha = 2.303A/d$ , where  $d$  is the sample thickness.

Optical energy gap  $E_g^{opt.}$  was computed using formula [27, 28]  $\alpha h\nu = B(h\nu - E_g^{opt.})^r$ , where  $B$  is a constant,  $h\nu$  indicates the photon energy,  $E_g^{opt.}$  is the optical energy gap;  $r = 3$  corresponds to the forbidden indirect transition and  $r = 2$  corresponds to the allowed indirect transition.

Refractive index ( $n$ ) was computed using formula [29]

$$n = \sqrt{4R - \frac{k^2}{(R-1)^2} - \frac{R+1}{R-1}},$$

where  $R$  is a reflection,  $k = \alpha\lambda/(4\pi)$  is an extinction coefficient,  $\lambda$  is a wavelength.

Optical conductivity ( $\sigma_{opt.}$ ) was determined [30] as  $\sigma_{opt.} = \alpha nc/(4\pi)$ , where  $c$  is velocity of light.

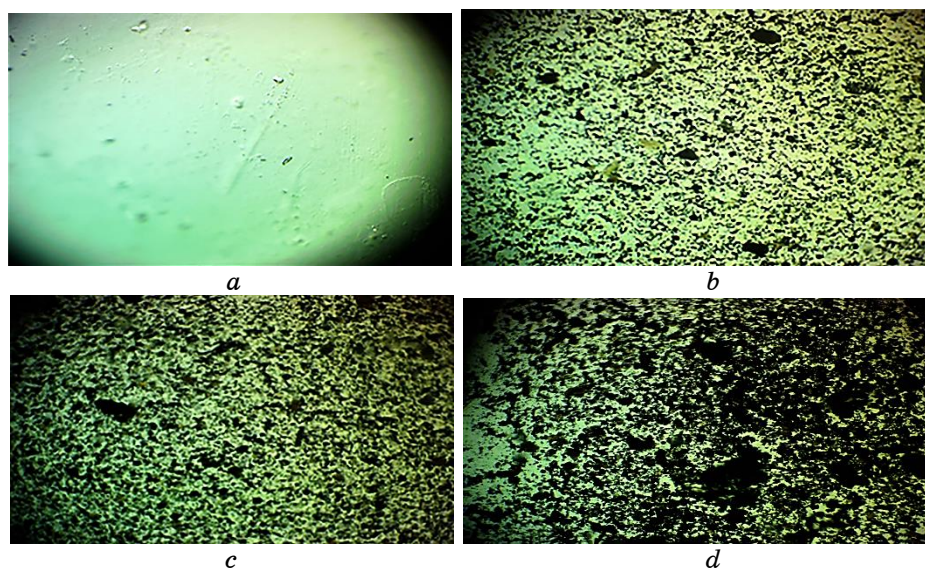


**Fig. 1.** Optical image of the film surface: (a) pure PVA; (b) PVA/(1% MnO<sub>2</sub>/1% SnO<sub>2</sub>); (c) PVA/(2% MnO<sub>2</sub>/2% SnO<sub>2</sub>); (d) PVA/(3% MnO<sub>2</sub>/3% SnO<sub>2</sub>).

### 3. RESULTS AND DISCUSSION

#### 3.1. Optical Image Analysis

Optical microscopy images of PVA, PVA/(1% MnO<sub>2</sub>/1% SnO<sub>2</sub>), PVA/(2% MnO<sub>2</sub>/2% SnO<sub>2</sub>), and PVA/(3% MnO<sub>2</sub>/3% SnO<sub>2</sub>) are shown in Fig. 1, *a–d*. The morphologies of the pure PVA film are illustrated in Fig. 1, *a*, which shows that its surface is so smooth and homogeneous [31]. As seen in Figs. 1, *b–d*, the optical microscopy images of PVA/MnO<sub>2</sub>/SnO<sub>2</sub> upon incorporation of MnO<sub>2</sub>/SnO<sub>2</sub> indicate the production of obvious spots with the creation of clear tiny aggregates, indicating the development of MnO<sub>2</sub>/SnO<sub>2</sub> in the PVA matrix. Discrepancy in surface morphologies detected upon introduction of MnO<sub>2</sub> can be attributed to the effective dispersing of MnO<sub>2</sub> within the PVA [32].

#### 3.2. FTIR Analysis

To study the physicochemical reactions and bonds between PVA and SnO<sub>2</sub>/MnO<sub>2</sub>, FTIR has been used. For this purpose, Figs. 2, *a–d* illustrate transmission spectrum *versus* the change in wave number; here, there are many peaks related to the different intensities and measurements related to the polymer and additives and their inter-

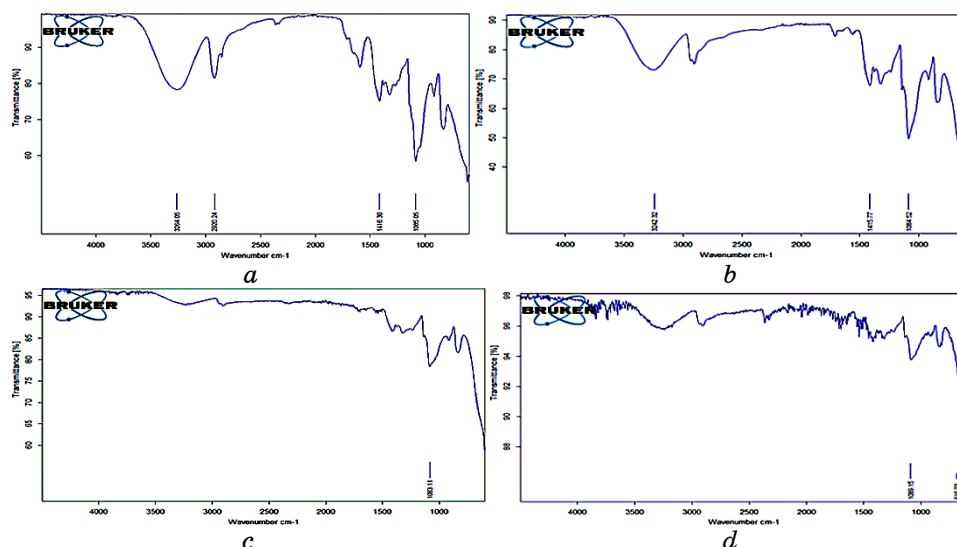


Fig. 2. Spectrum of FTIR for: (a) pure PVA; (b) PVA/(1% MnO<sub>2</sub>/1% SnO<sub>2</sub>); (c) PVA/(2% MnO<sub>2</sub>/2% SnO<sub>2</sub>); (d) PVA/(3% MnO<sub>2</sub>/3% SnO<sub>2</sub>).

actions [33]. The FTIR for PVA and the PVA/(SnO<sub>2</sub>/MnO<sub>2</sub>) composite are given in Figs. 2, *a–d*. The broad peaks at 3264 cm<sup>-1</sup> and 3242 cm<sup>-1</sup> are related to –OH groups, and peak at 2020 cm<sup>-1</sup> is due to stretching vibrations [34].

Another peaks at 1415 cm<sup>-1</sup>, 1416 cm<sup>-1</sup>, 1065 cm<sup>-1</sup>, 1083 cm<sup>-1</sup>, 1084 cm<sup>-1</sup>, and 1089 cm<sup>-1</sup> are referred to vibrations of –OH and C=O, respectively. The bands of 616 cm<sup>-1</sup> and 606 cm<sup>-1</sup> are referred to CH<sub>2</sub> stretches. Due to the interaction between MnO<sub>2</sub>, SnO<sub>2</sub> with PVA, these peaks were seen in all spectra with a slightly shift [35].

### 3.3. UV–Vis Spectrum Analysis

The absorbances of PVA before and after modification with SnO<sub>2</sub>/MnO<sub>2</sub> were plotted as a function of wavelengths as obvious in Fig. 3; it has been noticed that the absorbance is increasing with the increasing of the SnO<sub>2</sub>/MnO<sub>2</sub> ratio, and there is clearly absorption band at 340 nm, which is generally broadened and overlap so that the nanoparticles absorb light through these specific wavelengths [36, 37].

The variation of absorption coefficient  $\alpha$  of PVA before and after hybridization with SnO<sub>2</sub>/MnO<sub>2</sub> is shown in Fig. 4. The values of absorption coefficient  $\alpha$  for all samples were found to be greater than 10<sup>4</sup> cm<sup>-1</sup> in the near visible region; this means that they have direct optical energy gap, as illustrated in Fig. 5. It has been noticed that

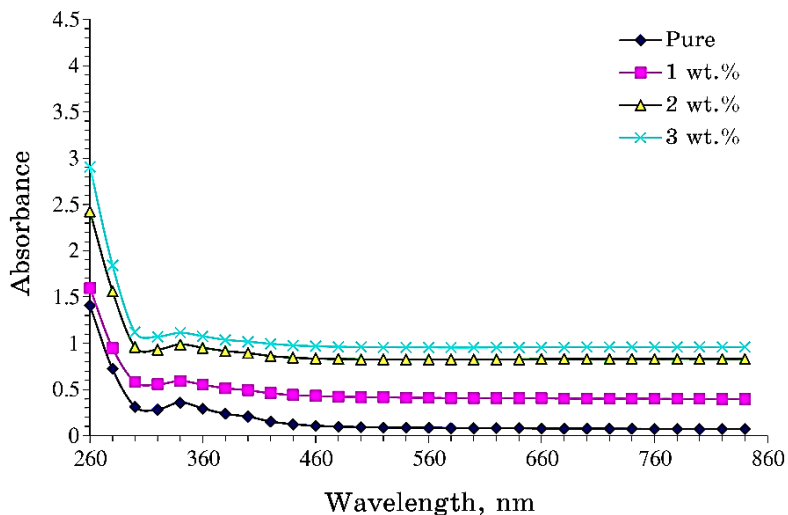


**Fig. 3.** Absorption as a function of wavelengths for pure PVA, PVA/(1% MnO<sub>2</sub>/1% SnO<sub>2</sub>), PVA/(2% MnO<sub>2</sub>/2% SnO<sub>2</sub>), PVA/(3% MnO<sub>2</sub>/3% SnO<sub>2</sub>).

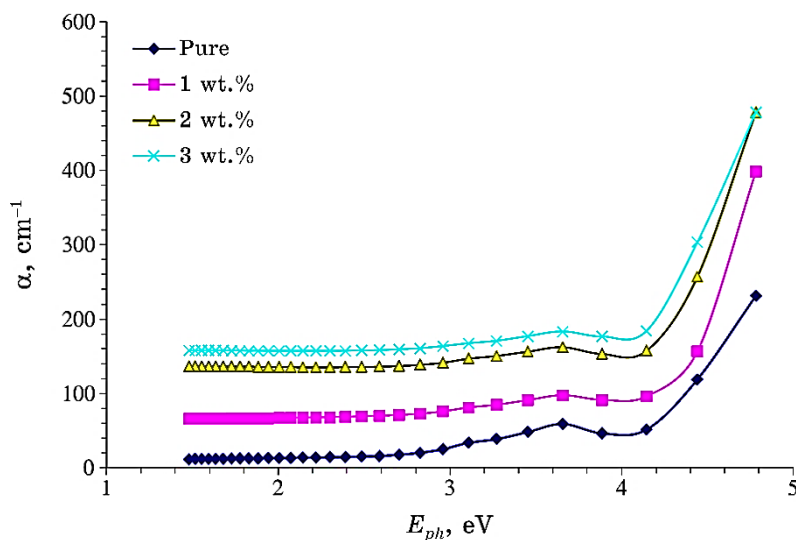


**Fig. 4.** Absorption coefficient as a function of photon energy for pure PVA, PVA/(1% MnO<sub>2</sub>/1% SnO<sub>2</sub>), PVA/(2% MnO<sub>2</sub>/2% SnO<sub>2</sub>), PVA/(3% MnO<sub>2</sub>/3% SnO<sub>2</sub>).

the value of absorption coefficient  $\alpha$  are increasing with the increase of SnO<sub>2</sub>/MnO<sub>2</sub> nanoparticles [38].

Figure 5 shows the result of  $(\alpha h\nu)^2$  versus  $h\nu$  to estimate the band gap of PVA and PVA/(MnO<sub>2</sub>/SnO<sub>2</sub>); it has been noticed that, when

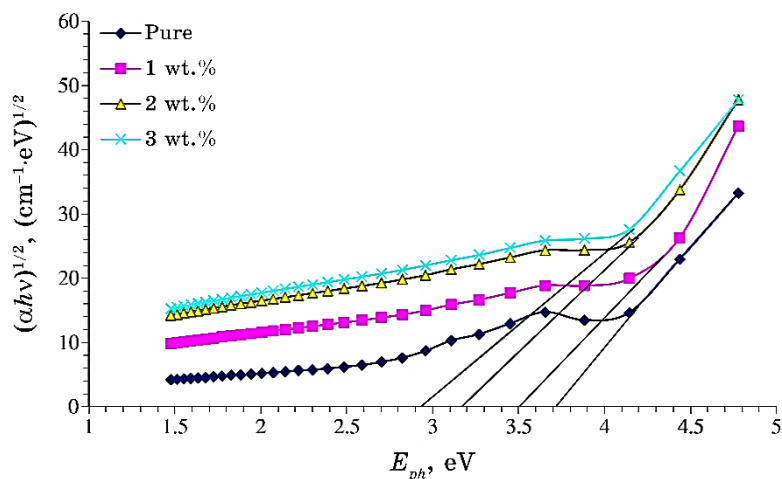


**Fig. 5.** Direct energy gap as a function of photon energy for pure PVA, PVA/(1% MnO<sub>2</sub>/1% SnO<sub>2</sub>), PVA/(2% MnO<sub>2</sub>/2% SnO<sub>2</sub>), PVA/(3% MnO<sub>2</sub>/3% SnO<sub>2</sub>).

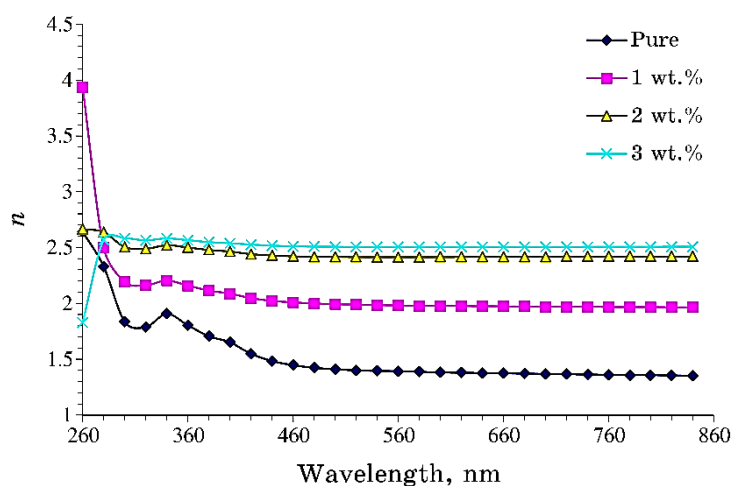


**Fig. 6.** Refractive index as a function of wavelengths for pure PVA, PVA/(1% MnO<sub>2</sub>/1% SnO<sub>2</sub>), PVA/(2% MnO<sub>2</sub>/2% SnO<sub>2</sub>), PVA/(3% MnO<sub>2</sub>/3% SnO<sub>2</sub>).

PVA is combined with MnO<sub>2</sub>/SnO<sub>2</sub> amounts, the band gap decreases from 3.73 eV for PVA to 3.62 eV, 3.19 eV, and 2.95 eV for PVA/1% wt./(MnO<sub>2</sub>/SnO<sub>2</sub>), PVA/2% wt./(MnO<sub>2</sub>/SnO<sub>2</sub>), and PVA/3% wt./(MnO<sub>2</sub>/SnO<sub>2</sub>), respectively. The adding of MnO<sub>2</sub>/SnO<sub>2</sub> nanoparticles to PVA causes flaws and link breakage, which contributes to the observed decrease in  $E_g$  [39].

Figure 6 shows refractive index for PVA before and after combi-

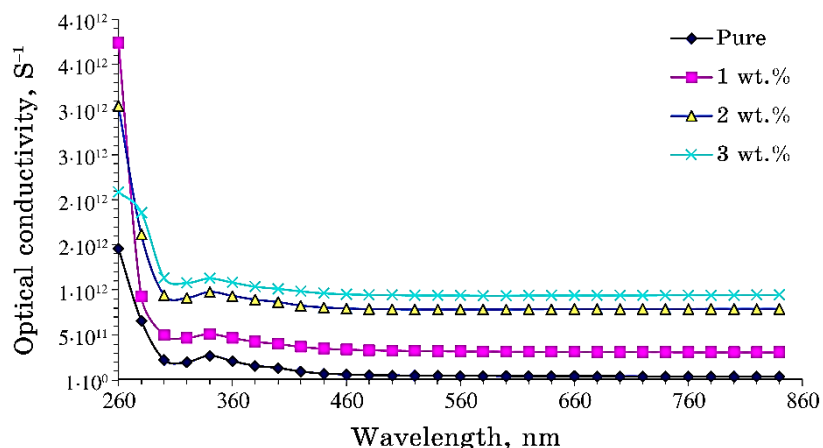


**Fig. 7.** Optical conductivity as a function of wavelengths for pure PVA, PVA/(1% MnO<sub>2</sub>/1% SnO<sub>2</sub>), PVA/(2% MnO<sub>2</sub>/2% SnO<sub>2</sub>), PVA/(3% MnO<sub>2</sub>/3% SnO<sub>2</sub>).

nation with SnO<sub>2</sub>/MnO<sub>2</sub> nanoparticles. In this figure, it has been noticed that the refractive-index values for PVA are increased with increasing of the ratio of SnO<sub>2</sub>/MnO<sub>2</sub> nanoparticles. Because of its low transmittance, the UV region has high refractive-index values, while the visible range has little ones.

The measured values of optical conductivity for PVA before and after modification with SnO<sub>2</sub>/MnO<sub>2</sub> are illustrated in Fig. 7, where the optical conductivity depends on the energy of the incident photons; it will be increased with the increase of photon energy because electrons can pass the valence band-to the local levels-to the conduction band more easily thanks to these new levels in this band gap. The band gap closes as a consequence and conductivity rises [42, 43].

#### 4. CONCLUSION

FTIR results show that PVA/MnO<sub>2</sub>/SnO<sub>2</sub>-nanocomposite films were successfully prepared in the present work. The results show that no chemical interaction between PVA and nanoparticles. Meanwhile, the absorbance, absorption coefficient, refractive index, optical conductivity, and optical band gap of PVA and PVA/MnO<sub>2</sub>/SnO<sub>2</sub> are determined.

The addition of MnO<sub>2</sub>/SnO<sub>2</sub> causes clear defects that leads to made a shift in the band gap. The results revealed that combination of MnO<sub>2</sub>/SnO<sub>2</sub> with PVA leads to enhancement of the optical characteristics that could lead to the usage of flexible PVA/MnO<sub>2</sub>/SnO<sub>2</sub> nanocomposite in a wide spectrum of potential devices.

## REFERENCES

1. V. M. Mohan, P. B. Bhargav, V. Raja, A. K. Sharma, and V. V. R. Narasimha Rao, *Soft Materials*, **5**, No. 1: 33 (2007); <https://doi.org/10.1080/15394450701405291>
2. Shaimaa Mazhar Mahdi and Majeed Ali Habeeb, *Optical and Quantum Electronics*, **54**: Article No. 854 (2022); <https://doi.org/10.1007/s11082-022-04267-6>
3. R. Tintu, K. Saurav, K. Sulakshna, V. P. N. Nampoori, P. Radhakrishnan, and S. Thomas, *J. Nan. Oxide Glas.*, **2**, No. 4: 167 (2010).
4. M. A. Habeeb and Z. S. Jaber, *East European Journal of Physics*, **4**: 176 (2022); doi:10.26565/2312-4334-2022-4-18
5. M. A. Habeeb, *European Journal of Scientific Research*, **57**, No. 3: 478 (2011).
6. Q. M. Jebur, A. Hashim, and M. A. Habeeb, *Egyptian Journal of Chemistry*, **63**: 719 (2020); <https://dx.doi.org/10.21608/ejchem.2019.14847.1900>
7. S. Ganeshan, P. Ramasundari, A. Elangovan, G. Arivazhagan, and R. Vijayalakshmi, *Int. J. Sci. Res. Phys. Appl. Sci.*, **5**, No. 6: 5 (2017); <https://doi.org/10.26438/ijrps/v5i6.58>
8. A. H. Hadi and M. A. Habeeb, *Journal of Mechanical Engineering Research and Developments*, **44**, No. 3: 265 (2021); <https://jmerd.net/03-2021-265-274/>
9. N. Hayder, M. A. Habeeb, and A. Hashim, *Egyptian Journal of Chemistry*, **63**: 577 (2020); doi:10.21608/ejchem.2019.14646.1887
10. Shaimaa Mazhar Mahdi and Majeed Ali Habeeb, *Polymer Bulletin*, **80**, No. 12: 12741 (2023); <https://doi.org/10.1007/s00289-023-04676-x>
11. M. A. Habeeb, A. Hashim, and N. Hayder, *Egyptian Journal of Chemistry*, **63**: 709 (2020); <https://dx.doi.org/10.21608/ejchem.2019.13333.1832>
12. A. Hashim, M. A. Habeeb, and Q. M. Jebur, *Egyptian Journal of Chemistry*, **63**: 735 (2020); <https://dx.doi.org/10.21608/ejchem.2019.14849.1901>
13. S. M. Mahdi and M. A. Habeeb, *Physics and Chemistry of Solid State*, **23**, No. 4: 785 (2022); doi:10.15330/pcss.23.4.785-792
14. Nawras Karim Al-Sharifi and Majeed Ali Habeeb, *Silicon*, **15**: 4979 (2023); <https://doi.org/10.1007/s12633-023-02418-2>
15. Majeed Ali Habeeb and Waleed Shaker Mahdi, *International Journal of Emerging Trends in Engineering Research*, **7**, No. 9: 247 (2019); doi:10.30534/ijeter/2019/06792019
16. M. A. Habeeb and R. S. Abdul Hamza, *Journal of Bionanoscience*, **12**, No. 3: 328 (2018); <https://doi.org/10.1166/jbns.2018.1535>
17. Ahmed Hashim, Alaa J. Kadham Algidsawi, Hind Ahmed, Aseel Hadi, and Majeed Ali Habeeb, *Nanosistemi, Nanomateriali, Nanotehnologii*, **19**, Iss. 2: 353 (2021); <https://doi.org/10.15407/nnn.19.02.353>
18. M. A. Habeeb, A. Hashim, and N. Hayder, *Egyptian Journal of Chemistry*, **63**: 697 (2020); <https://dx.doi.org/10.21608/ejchem.2019.12439.1774>
19. M. A. Habeeb and W. K. Kadhim, *Journal of Engineering and Applied Sciences*, **9**, No. 4: 109 (2014); doi:10.36478/jeasci.2014.109.113
20. Alaa Abass Mohammed and Majeed Ali Habeeb, *Silicon*, **15**: 5163 (2023); <https://doi.org/10.1007/s12633-023-02426-2>
21. M. A. Habeeb, *Journal of Engineering and Applied Sciences*, **9**, No. 4: 102

- (2014); doi:10.36478/jeasci.2014.102.108
22. Ahmed Hashim, Alaa J. Kadham, Aseel Hadi, and Majeed Ali Habeeb, *Nanosistemi, Nanomateriali, Nanotehnologii*, **19**, Iss. 2: 327 (2021); <https://doi.org/10.15407/nnn.19.02.327>
  23. S. M. Mahdi and M. A. Habeeb, *Digest Journal of Nanomaterials and Biostructures*, **17**, No. 3: 941 (2022); <https://doi.org/10.15251/DJNB.2022.173.941>
  24. Ahmed Hashim, Alaa J. Kadham Algidsawi, Hind Ahmed, Aseel Hadi, and Majeed Ali Habeeb, *Nanosistemi, Nanomateriali, Nanotehnologii*, **19**, Iss. 1: 91 (2021); <https://doi.org/10.15407/nnn.19.01.091>
  25. Araa Hassan Hadi and Majeed Ali Habeeb, *Journal of Physics: Conference Series*, **1973**, No. 1: 012063 (2021); doi:10.1088/1742-6596/1973/1/012063
  26. Q. M. Jebur, A. Hashim, and M. A. Habeeb, *Egyptian Journal of Chemistry*, **63**, No. 2: 611 (2020); <https://dx.doi.org/10.21608/ejchem.2019.10197.1669>
  27. C. Uma Devi, A. K. Sharma, and V. V. R. N. Rao, *Materials Letters*, **56**, No. 3: 167 (2002); [https://doi.org/10.1016/S0167-577X\(02\)00434-2](https://doi.org/10.1016/S0167-577X(02)00434-2)
  28. Majeed Ali Habeeb and Ahmed Hashim Mohammed, *Optical and Quantum Electronics*, **55**: Article No. 791 (2023); <https://doi.org/10.1007/s11082-023-05061-8>
  29. M. H. Dwech, M. A. Habeeb, and A. H. Mohammed, *Ukr. J. Phys.*, **67**, No. 10: 757 (2022); <https://doi.org/10.15407/ujpe67.10.757>
  30. Rehab Shather Abdul Hamza and Majeed Ali Habeeb, *Optical and Quantum Electronics*, **55**: Article No. 705 (2023); <https://doi.org/10.1007/s11082-023-04995-3>
  31. Alaa J. Kadham Algidsawi, Ahmed Hashim, Aseel Hadi, Majeed Ali Habeeb, and Hussein Hakim Abed, *Physics and Chemistry of Solid State*, **23**, No. 2: 353 (2022); <https://doi.org/10.15330/pcss.23.2.353-360>
  32. Majeed Ali Habeeb and Waleed Hadi Rahdi, *Optical and Quantum Electronics*, **55**: Article No. 334 (2023); <https://doi.org/10.1007/s11082-023-04639-6>
  33. H. N. Chandrakala, B. Ramaraj, Shivakumaraiah, G. M. Madhu, and Siddaramaiah, *Journal of Alloys and Compounds*, **551**: 531 (2013); <https://doi.org/10.1016/j.jallcom.2012.10.188>
  34. A. Hashim and M. A. Habeeb, *Journal of Bionanoscience*, **12**, No. 5: 660 (2018); <https://doi.org/10.1166/jbns.2018.1578>
  35. Shaimaa Mazhar Mahdi and Majeed Ali Habeeb, *AIMS Materials Science*, **10**, No. 2: 288 (2023); doi:10.3934/matricsci.2023015
  36. J. Selvi, S. S. Mahalakshmi, and V. Parthasarathy, *J. Inorg. Organomet. Polym. Mater.*, **27**: 1918 (2017); <https://doi.org/10.1007/s10904-017-0662-1>
  37. Nawras Karim Al-Sharifi and Majeed Ali Habeeb, *East European Journal of Physics*, **2**: 341 (2023); doi:10.26565/2312-4334-2023-2-40
  38. A. J. K. Algidsawi, A. Hashim, A. Hadi, and M. A. Habeeb, *Semiconductor Physics, Quantum Electronics and Optoelectronics*, **24**, No. 4: 472 (2021); <https://doi.org/10.15407/spqeo24.04.472>
  39. Nhiem Tran, Aparna Mir, Dhriti Mallik, Arvind Sinha, Suprabha Nayar, and Thomas J Webster, *Int. J. Nanomedicine*, **5**: 277 (2010); <https://doi.org/10.2147/IJN.S9220>
  40. Zainab Sabry Jaber, Majeed Ali Habeeb, and Waleed Hadi Radi, *East European Journal of Physics*, **2**: 228 (2023); doi:10.26565/2312-4334-2023-2-25

41. M. A. Habeeb and R. S. A. Hamza, *Indonesian Journal of Electrical Engineering and Informatics*, **6**, No. 4: 428 (2018); doi:10.11591/ijeei.v6i1.511
42. A. A. Mohammed and M. A. Habeeb, *East European Journal of Physics*, **2**: 157 (2023); doi:10.26565/2312-4334-2023-2-15
43. O. E. Gouda, S. F. Mahmoud, A. A. El-Gendy, and A. S. Haiba, *Indonesian Journal of Electrical Engineering*, **12**, No. 12: 7987 (2014); <https://doi.org/10.11591/telkomnika.v12i12.6675>